

IN-PROCESS MEASUREMENT OF BENDING ANGLES BASED ON THE PRINCIPLE OF LIGHT SECTIONING

Dipl.-Phys. Werner Heckel
Scientific Assistant

University of Erlangen-Nürnberg, Chair of Manufacturing Technology
Univ.-Prof. Dr.-Ing. M. Geiger, Egerlandstr. 11, D-8520 Erlangen, Tel. +49/9131/85-7140
Germany

ISPRS Commission V

ABSTRACT:

This paper presents an industrial application of optical 3-D sensing based on the principle of light sectioning. The presented project aims at an in-process measurement of the bending angle in a commercial bending machine. Air bending is a valuable manufacturing method in a flexible and computer integrated manufacturing system, because it allows forming of sheet metals with a great variety of bending angles. But achieving high working accuracies requires adaptive control strategies to overcome deviations from the desired bending angle caused by material tolerances.

The investigations comprise fundamentals of system design for integrating such a measuring system in any commercial bending machine. System design considerations about the choice of the components and synchronization of illumination and detection system are described. Furthermore, the different steps for achieving 3-D data are sketched. First step is evaluating the position of the profile on the CCD sensor with subpixel accuracy due to interpolation algorithms. Next step is the calculation of 3-D coordinates which correspond to these sensor positions.

The bending angle can be evaluated with statistical deviations of about 1 angular minute. But measuring absolute values of bending angles presupposes knowledge of the correspondence between camera and workpiece coordinates. The basic equations to describe this correspondence and the application of photogrammetric calibration methods for a simple model of the detection system are presented. First experimental results prove the derived equations and show promising results even for the simple model of the detection system.

KEY WORDS: 3-D, Image Processing, Machine Vision, System Design, Interpolation Algorithms, Subpixel Accuracy, Camera Calibration

INTRODUCTION

Modern manufacturing systems have to deal with the requirements of 'just-in-time' manufacturing, i.e. flexible manufacturing of a great variety of parts with very small lot sizes. Air bending allows forming of sheet metals with a great variety of bending angles without tool changes and is therefore a valuable manufacturing method for flexible and computer integrated manufacturing systems.

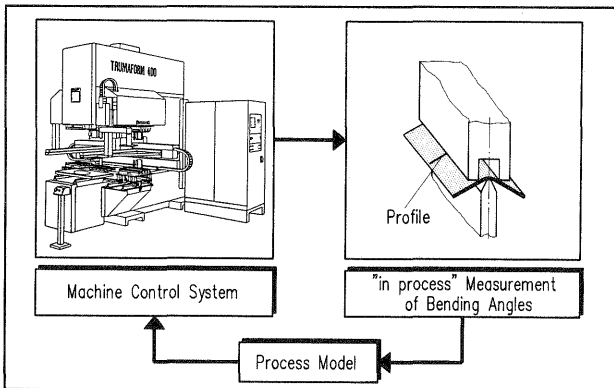


Fig. 1: Adaptive control system for air bending

In spite of high precision control systems for modern bending machines, material tolerances (for example sheet thickness, yielding point, anisotropy, etc.) cause deviations from the desired bending angle. Assuming the material tolerances as specified by sheet metal manufacturers, these deviations can amount up to 1,5°. This demands for adaptive control strategies to achieve a sufficient working accuracy. A simple adaptive control system for air bending is depicted schematically in Fig. 1. The fundamental component of this adaptive control system is an in-process measuring system for the bending angle. But knowing the in-process bending angle still requires modelling of the bending process, because the elastic resiliency of the workpiece has to be compensated.

Thus the presented project aims at the development of an measuring system for in-process measurement of bending angles. The primary investigations should evaluate fundamentals of system design for the integration of this in-process measuring system in any commercial bending machine. The selected 3D-sensing system bases on the well-known triangulation principle of light sectioning. This non-contact, simple, fast and precise optical 3-D measuring method meets

the requirements for an in-process measuring of bending angles.

THE PRINCIPLE OF LIGHT SECTIONING

In [1] the principle of a modified light sectioning system with large depth and high resolution was reported. There an axicon [2],[3] was used to overcome the depth of focus problem. Scanning the diffraction pattern of an axicon produces a thin, deep light sheet, which results from the incoherent superposition of axicon patterns along the scanner path. This so-called 'light knife' allows sharp illumination of an object within a longitudinal range of typ. 1500 mm. With a detector design regarding to the Scheimpflug condition (see for example [4]) sharp imaging of the object all over the range of the 'light knife' can be achieved. Thus a 3-D sensor with high resolution and nearly unlimited depth of focus could be constructed.

The reported 3-D sensing method for measuring bending angles is based mainly on the same principle, as it is shown in Fig. 2.

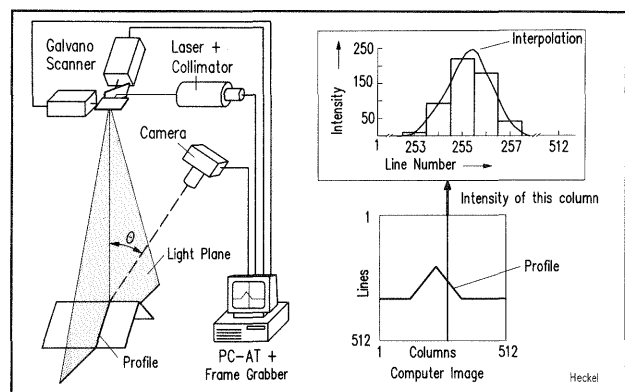


Fig. 2: Principle of Light Sectioning

The bending angle usually refers to the original state of a plane sheet metal. Hence the bending angle is 180°-complementary to the angle between the two legs of the bent workpiece. These legs have only very small curvature, which reduces the demands for lateral resolution of the measuring system. Furthermore, evaluation of a profile includes interpolation algorithms to calculate the center of the intensity distribution of the profile. Therefore slightly defocused profiles are acceptable and laser beam focusing with a spherical lens is sufficient. This avoids some drawbacks of axicons, like for example

limited diffraction efficiency, disturbance of the profiles caused by diffraction rings and difficult and expensive manufacturing of an axicon.

For that reasons a commercial available laser diode with collimator optics is used for illumination. The focused laser beam is scanned over the object with a two-axis galvanometric scanner, which spans up a light plane. The intersection of light plane and workpiece surface, the so-called 'profile', is detected with a CCD TV-camera under the triangulation angle θ . All components are connected to a PC-AT computer, which controls the whole system and evaluates the bending angle from the camera picture stored in a frame grabber.

The 3-D coordinates of the workpiece surface are coded in the position of the image of 'profile' on the CCD sensor, respectively in the frame grabber coordinates of the profile. In the dimension across the profile these coordinates can be evaluated with very high precision by means of interpolation algorithms. Looking at the intensity distribution in Fig. 2 one can imagine the interpolation procedure:

First the computer searches in each vertical column (resp. horizontal line) of the frame grabber for the pixel with maximum intensity, assuming it to be an approximate position of the profile. The interpolation function (for example a Gaussian distribution curve) is fitted through the intensity distribution of the highest pixel and its neighbourhood. The calculated center position of the fitted curve is interpreted as subpixel position of the profile in this column (resp. line) of the computer image.

Hence evaluation of one picture of the CCD TV-camera delivers 3-D coordinates of typically 500 spots on the workpiece surface along the scanner path. Each of the legs of the workpiece is represented by a straight line of measuring spots and the bending angle is complementary to the angle between these two lines. Linear regression analysis allows calculation of this angle with very high precision and simultaneously statistical predictions about the performance of the measuring system.

SYSTEM DESIGN

The investigations of system design fundamentals for integration in commercial bending machines are undertaken with an off-line measuring system to provide necessary flexibility. Fig. 3 schematically shows the experimental setup for this off-line measuring system.

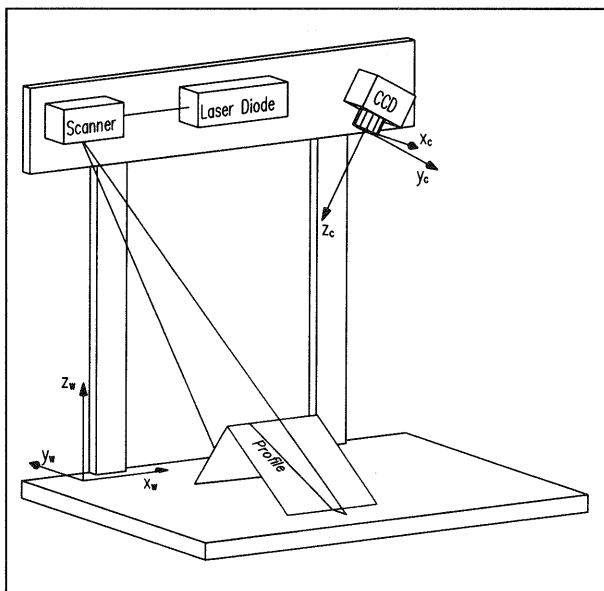


Fig. 3: Experimental Setup

All components are fixed to a three dimensional 'optical bench'. The optical bench consists of a plane table for the positioning of the workpiece and a height-adjustable cross-head onto which the components of the measuring system are fixed. Spe-

cial mechanical adapters allow simple but reproducible shifting of laser, scanner and camera along a common optical axis. Furthermore, the adapter of the camera allows turning the camera around the principal point of its objective. The host computer (PC-AT) controls and synchronizes all components of the measuring system, evaluates 3-D coordinates of the 'profile' and calculates the bending angle from this information. First some system design considerations about the choice of the main components of the system are discussed. Synchronization of the components and evaluation of 3-D data will be discussed in consecutive chapters.

Illumination of the object

The illumination system consists of a laser diode ($\lambda = 789 \text{ nm}$, $P_0 = 30 \text{ mW}$) which is focused on the workpiece surface by a collimator, consisting of a lens doublet ($f = 90 \text{ mm}$, $n.A. = 0,17$), which is corrected for aperture aberrations. This collimator was primary designed for homogenous illumination of a circular field of 30 mm in diameter. The great astigmatism of laser diodes is diminished by internal diaphragms, which cause loss of effective output power. Here the collimator is adjusted to a focus distance of 1100 mm (instead of a parallel beam) to avoid an additional focusing lens. This adjustment increases distance from laser diode to collimator lens and causes additional internal absorption. Hence the effective output power of the collimated laser beam decreases to about 9 mW.

The generation of a light plane or 'light knife' from the focused laser beam is done by a two-axis galvanometric scanner. This scanner allows beam deflections up to $\pm 20^\circ$ (optical) with frequencies up to 80 Hz. Each dimension of the scanner field is divided into 65535 possible scanner addresses (16 bit). Scanner electronics are programmed via a parallel (Centronics) interface and include its own microprocessor to calculate flat-field corrected 'micro-steps' of the scanner motion. Scanner electronics independently switch laser power on and off via a TTL interface to the laser power supply.

Detection of the profile

The detection of the profile is done with a CCD TV camera. Reasons for the choice of this type of detector are the well-known advantages of CCD sensors like, for example, precise and stable sensor geometry [5], high resolution and high light sensitivity. The aim of integrating the measuring system in industrial bending machines furthermore emphasizes the features of light weight, resistance to mechanical shocks or magnetic fields and low costs. These considerations also suggest the use of a camera with separate sensor head (size 44 x 31 x 25 mm³, weight 80 g). To eliminate ambient light in an industrial environment a band-pass interference filter is built into the camera.

SYNCHRONIZATION OF COMPONENTS

The laser spot is moved over the workpiece surface during the comparatively short integration period of the detector. Hence a line of light is detected, the so-called 'profile', which, mathematically, is the intersection of the workpiece surface with the 'light knife'. For perfect exposure one scan of the laser beam must be detected by the CCD sensor in one frame.

Therefore illumination system (i.e. laser and scanner), CCD camera and image acquisition system have to be synchronized. The frame grabber automatically synchronizes to the camera's video cycle and the host computer's program execution is synchronized to the frame grabber. Hence the camera's video cycle is essential for synchronization of the whole measuring system. But integration timing of CCD cameras differs significantly with the sensor concept and a basic understanding of CCD sensor timing is necessary.

Synchronization of frame-transfer CCD cameras

Most wide-spread sensor concepts are frame-transfer-concept (FT) and interline-transfer-concept (IL). FT sensors have two sections of equal size, an imaging area and a read-out area. In the imaging

area incoming photons generate electrons, which are integrated in CCD registers. These charge packets represent the picture information. After the integration period of approx. 20 ms (CCIR standard), all charge packets of this field are shifted into the light-shielded read-out area. During this 'frame-transfer' period (of about 1 ms) generation of electrons by incoming photons is still going on and high intensity spots in the image will cause evident 'smear' effects. During the integration period of the next field the video signal of the previous field is generated line by line from the charge packets in the light-shielded read-out area. Hence the two interlaced fields of a frame are integrated in a completely sequential manner.

The following aspects are essential for synchronization of FT cameras to scanning or flashlight illumination systems:

- The two fields of a frame are integrated in a total sequential order. At no times both fields of a frame can be exposed simultaneously. As a consequence the spatial resolution of the detector is approximately halved, because information from one scan over the object can be detected only in one field. Exposing a frame would require two separate scans, which might cause reproducibility problems.
- The scanned laser beam is a very intensive light source. So accidental scanning during frame transfer period will cause severe smear effects. These smear effects can be avoided by an additional shutter, which shields the sensor from light during frame-transfer periods.
- These drawbacks of FT sensors for use in systems with flash illumination should be carefully compared to the advantages of FT sensors like, for example, higher light sensitivity and full area fill factor of light sensitive regions.

Fig. 4 shows a distinguished example for smear effects caused by scanning the laser beam during a frame-transfer period. In reality the laser beam is

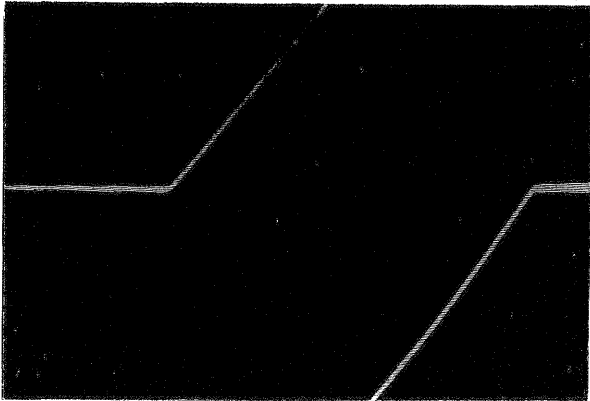


Fig. 4: Example for smear effects using a frame-transfer CCD camera

scanned straight over the image from the right to the left side. This example shows a virtual bending of the trace of the laser beam caused by transportation of the image's charge packets over the bright laser spot during frame transfer. This explains easily the bending of the right line towards the bottom of the image. But the example shows two bent lines, one in each field of the same frame. The other line is bent towards the top of the image, which would conflict with the transfer direction in a simple explanation of smear effects. What is the reason for the astonishing smear effect shown in Fig. 4?

Fig. 5 depicts the position of several successive fields (represented physical as charge packets) on the sensor at selected moments of the sensor timing:

Time $t=T_1$ is near the end of the integration period. Integration of the first field is still going on and the laser beam is moving along the scanner path.

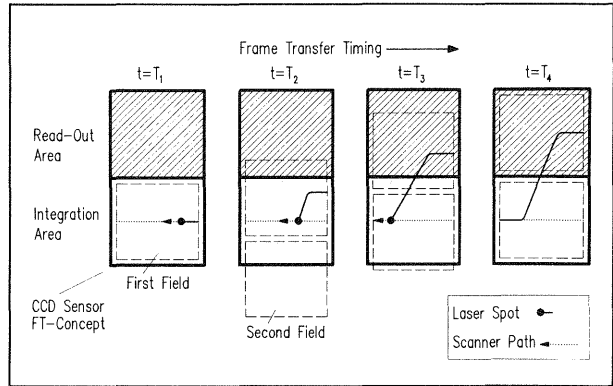


Fig. 5: Explanation of smear effects during frame transfer

At time $t=T_2$ frame transfer is in progress and the first field is to be transferred into the light-shielded read-out area. The scanned laser spot will still produce charge packets. Thus transfer motion will bend the trace of the laser beam towards the bottom of the field.

Time $t=T_3$ is just before end of transfer period and the first field is mostly transferred into the read-out area. Timing signals for charge packet transfer are fed on all picture elements of the integration area simultaneously. Therefore charge packets generated by the bright laser spot during the transfer process will also smear the next field (in advance of the normal integration period). Figuratively spoken, the next field seems to be drawn into the integration area coming from the bottom of the sensor. Hence the bent laser beam trace will continue at the top of the next field after it has reached the bottom of the first field.

At time $t=T_4$ the frame transfer process is completed. The first field is to be read out and the integration of the second field is in progress. Combining the two fields depicted at $t=T_4$ in Fig. 5 yields exactly to a frame with a smear effect as shown in Fig. 4.

Smear effects in such an evident manner occur only with stroboscopic illumination or very intense and fast moving light sources. Assuming one scan of the laser beam over 500 horizontal sensor elements during 20 ms, effective exposure time for one sensor element is only 40 μ s. Compared to that the frame transfer period is very long and smear effects become evident. Normally each sensor element integrates charge packets from a standing scene for an exposure time of 20 ms and the frame transfer period is comparatively short. In this case, smear effects get noticeable only in the surroundings of very bright light sources.

Synchronization of interline-transfer CCD cameras

The other wide-spread CCD sensor concept is the interline-transfer (IL) concept. In the IL-organization, each light-sensitive imaging column has an optical shielded column of vertical shift registers adjacent to it. Each pair of light sensitive sensor elements (one for each field) shares one common vertical shift register. The output cycle of IL-sensors starts with shifting charge packets of all even lines or all odd lines (alternating according to the CCIR interlace standard) into light shielded vertical shift registers. All charge packets are shifted at once, i.e. the transfer period of IL sensors lasts less than 1 μ s and is about 250 times shorter than that of FT sensors. Light protected vertical shift registers move the charge packets line by line into the horizontal shift register, from which the charge packets are read out and finally converted into CCIR standard video signals.

As a consequence, each sensor element collects photons for a frame period of approx. 40 ms. Sensor elements from even and odd lines are read out alternately with an interlace of a field period (20 ms). Will this timing give us a chance to expose a full frame with one single scan?

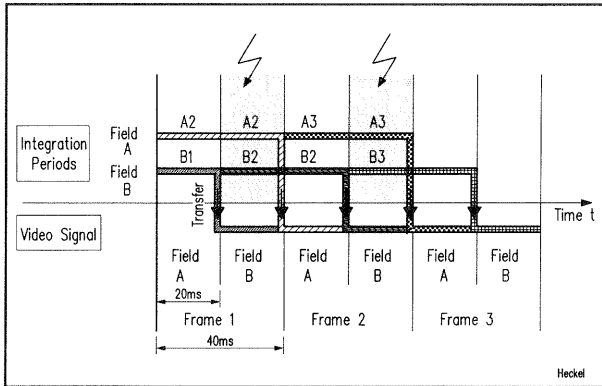


Fig. 6: Temporal interdependence of video signal and integration periods (IL-sensors)

Fig. 6 shows the temporal interdependence between the actual video signal and the integration period to which it belongs. The integration period for the video signal of a field are the two preceding fields. For example (see Fig. 6), the information of field B1 was integrated during the read-out periods of fields A1 and A2. At every time two consecutive fields are exposed simultaneously. Perfect exposure of the profile (with full spatial resolution) must take place during periods of simultaneous exposure of two fields (for example fields B1 and B2) belonging to the same frame (for example frame B). For every frame the period of simultaneous integration of both fields is the read-out period of the second field of the preceding frame. Exposures during this period will be integrated in both fields of the next frame. One scan in this period will be detected with full spatial resolution.

Hence the following aspects are essential for synchronization of IL cameras to systems with scanning illumination or flashlight illumination:

- The two fields of a frame are read out in an interlaced modus, but each sensor element integrates charge packets for a full frame period.
- During the read-out period of the second field of a frame both fields of the next frame are integrated simultaneously. If the scanner (resp. flashlight) is active during this period of approximately 20 ms, the next frame will contain one exposure with full spatial resolution.
- IL cameras will show only very little smear effects, even for accidental exposure during transfer periods.

For this reasons interline-transfer CCD cameras will be preferable detectors for use in systems with scanning or flashlight illumination.

Synchronization in the presented measuring system

The selected CCD camera (SONY XC 77 CE) is based on an interline-transfer sensor. Exposure of the object must take place during the integration period of any second field. The next frame of the video signal will contain the desired image and has to be captured by the frame grabber of the host computer. A reproducible relation between camera cycles, scanner motion and frame grabber is assured with the following procedure:

1) Generation of the scanner program:

Starting with user-defined coordinates for starting and final point of the scan vector the host computer calculates the scanner program in such manner, that the laser beam will move along the scan vector during the integration period of 20 ms. Different vector lengths will cause varying exposure of the profile. Later on this drawback will be abolished by controlling the laser power from host computer.

2) Programming the scanner unit:

The host computer programs the scanner electronics. The mirrors move to the starting point, the scanner unit stores the coordinates of the final point and waits for the execution command.

3) Synchronizing with camera timing:

The host computer waits for the next vertical blanking pulse (i.e. the beginning of the next full frame). Then it gives execution order for the scanner unit.

4) Scanning:

The scanner waits for the beginning of the second field (experimentally determined delay time). Then, after acceleration of the mirrors, the laser is switched on and the laser beam moves along the scan vector. The scanner electronics independently calculates flat-field corrected 'micro-steps' for the mirror motion.

5) Image acquisition:

The host computer grabs the next frame of the camera signal for evaluation in the frame storage.

With this procedure a correct exposure of a full frame is assured independent from length or position of the scan vector. Remember that the laser beam is switched on only for an exposure time of 20 ms, which reduces possible dangers of the invisible laser diode beam significantly.

EVALUATION OF PROFILE POSITIONS IN COMPUTER IMAGE

The position of the profile is evaluated in each vertical column (or horizontal line, depending on the direction of the profile) of the computer image with subpixel accuracy. Thus each column delivers one measuring point and each leg of the profile composes of about 200-250 data points for profile positions. Linear regression for each leg yields to predictions for the straight lines with statistical improved accuracy. For absolute measurements of bending angles the conclusion from profile's positions in computer image to 3-D coordinates of workpiece surface must be drawn.

Gaussian interpolation algorithm

Subpixel accuracy profile position in each column is achieved using interpolation algorithms. First the computer searches in each line resp. column of the computer image for the pixel with maximum intensity, assuming it to be an approximate position of the profile. An interpolation function is fitted through the intensity distribution of this pixel and its direct neighbours. The calculated center position of the interpolation function is interpreted as position of the profile in this line resp. column of the computer image. Hence the profile is now represented by 512 data points with subpixel accuracy.

A lot of interpolation algorithms have been discussed by different authors (see for example [6], [7], [13], [14], [15]). Interpolation algorithms based on Gaussian distribution curves are quite obvious, because the peak of almost every laser beam intensity distribution shows approximately Gaussian character. Eq. (1) denotes this assumption by

$$I(x) = A \cdot \exp\left(-\frac{(x-C)^2}{B}\right) \quad (1)$$

where:

$I(x)$ Gaussian intensity distribution
 A, B, C amplitude, width and center position of the Gaussian distribution curve.

The information from at least three pixels is necessary to calculate the three parameters A, B, C of the Gaussian interpolation curve. Let these three pixels be the pixel x_0 with maximum intensity I_0 and two of its neighbours (x_a, I_a) and (x_b, I_b) with $I_a < I_0$ and $I_b < I_0$. Essential for calculating profile positions is only the center position C of the Gaussian distribution curve, which is determined by Eq. (2)

$$C = \frac{(x_b - x_0) \frac{L-R^2}{L-R}}{2} \quad \text{with } L = \frac{\ln(I_0/I_a)}{\ln(I_0/I_b)} \quad (L \neq R) \quad (2)$$

$$\text{and } R = \frac{x_a - x_0}{x_b - x_0}$$

which reduces for the usual case of adjacent pixels ($x_a - x_0 = -1$ and $x_b - x_0 = +1$) to Eq.(3) for the subpixel center position C of the Gaussian distribution curve

$$C = \frac{L-1}{2(L+1)} \quad (3)$$

Gaussian interpolation proved to be a very effective and precise subpixel accuracy algorithm. It is more precise than simple centroid calculation, where especially the choice of the evaluated pixel range is very critical. Gaussian interpolation needs not too much calculation efforts, but proved to be a resistant algorithm with little systematic errors of about 1% of a pixel period [8].

Linear regression analysis

Next step for evaluating the bending angle is separation of the two legs of the profile and linear regression in each leg. Regression analysis will give improved values for the slopes of the two legs of the profile and, simultaneously, statistical prediction for the resolution of the measuring system.

EVALUATION OF 3-D COORDINATES

For evaluation of the bending angle the relations between 3-D coordinates of the workpiece surface and profile positions in computer image have to be known. Only an exact knowledge of this relations gives the chance to evaluate the bending angle of a workpiece from the profile in the computer image. The functional relations become calculable by performing all coordinate transformations through the detection system. But the equations contain a lot of parameters (for example internal and external camera parameters, lens distortion, digital image acquisition parameters), most of which can not be measured directly. These parameters have to be calibrated, which is a familiar procedure in close range photogrammetry (see for example [9]). In the following the functional relation of 2-D computer image coordinates and 3-D workpiece coordinates are to be evaluated.

3-D sensing by triangulation is based on calculating the intersection point of two rays in space. One of these two rays is given by the direction of illumination. However, in our system not a ray but a light plane is defined by the scanner path. The intersection of this light plane with the object's surface yields to the 'profile' of the object. Hence the coordinates of the light plane give a first geometric locus for the surface of the workpiece.

Transforming back one profile position in the computer image through all steps of the detection system provides 3-D coordinates of a ray, on which one spot of the profile must lie. This ray gives the second geometric locus for one point of the workpiece surface.

World coordinate system

First step is definition of a 3-D world coordinate system, to which all other coordinate systems refer. In this system the bending angle has to be calculated finally.

The schematical drawing of the experimental setup in Fig. 3 depicts also the cartesian world coordinate system $\{x_w, y_w, z_w\}$ and the camera coordinate system $\{x_c, y_c, z_c\}$. The origin of world coordinates is defined by the point of impact of the laser beam in the center of the scanner coordinate system. x_w and y_w -axes lie on top of the table and are parallel to the corresponding axes of the scanner coordinate system. z_w -dimension is the height above the table. To get a right-handed world coordinate system the y_w -axis has opposite direction than y_s -axis, hence $y_w = -y_s$.

Camera coordinate system

The z_c -axis of the camera coordinate system is given by the optical axis of the imaging system. The origin lies in the principal point of the objective and the y_c -axis is assumed parallel to the $-(y_w)$ -

axis. Due to the opposite direction of y_w and y_c the y_w -axis is aligned with the corresponding frame storage axis y_f . The translation vector of the camera system is $T(t_x, t_y, t_z)$, the rotational orientation may be denoted, for example, by the direction cosines between the axes of the coordinate systems.

Scanner coordinate system

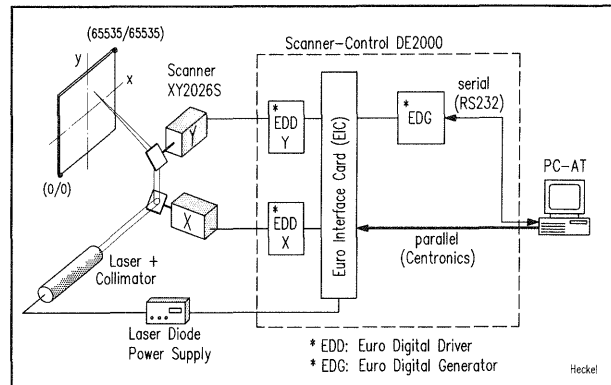


Fig. 7: Components of illumination system

Fig. 7 shows the components of the illumination system and illustrates definition of the scanner coordinate system. The scanner electronics address the working field of the scanner (maximum deviation angle $\Phi_{x,y}$ can be adjusted up to $\pm 20^\circ$ optical) by 16 bit integers, i.e. scanner coordinates stretch from 0 to 65535 LSB (Least Significant Bit) in each dimension. The center of the scanner working field is addressed by the scanner coordinates $(x,y)_s = (32767, 32767)$.

Correspondence between world coordinates and scanner coordinates is simplified by the intrinsic geometric flat-field correction of the scanner electronics. The scanner program generated by the host computer is sent to the 'Euro Digital Generator' (EDG) via a standard 'Centronics' interface. The EDG stores and executes the scanner program independently. During scan vector processing the EDG calculates 'micro-steps' every 150 μs and sends them to the 'Euro Digital Drivers' (EDD), which control the movement of the x- and y-mirrors. The EDG calculates flat-field corrected micro-steps based on a stored grid correction table, which is specific for each working distance and scanner configuration.

Hence the relation of scanner coordinates and world coordinates on the surface of the table ($z_w=0$) is simply given by the linear transformation of Eq. (4)

$$\begin{pmatrix} x \\ y \\ z \end{pmatrix}_w = \begin{pmatrix} \frac{x_s - 32767}{32767} \cdot d_s \cdot \tan(\Phi_x) \\ -\frac{y_s - 32767}{32767} \cdot d_s \cdot \tan(\Phi_y) \\ 0 \end{pmatrix} \quad (4)$$

where

d_s working distance (from the last scanner mirror to the optical table)

$\Phi_{x,y}$ maximum scan angle in x_w, y_w direction

World coordinates of the light plane

The light plane is defined by three outstanding points in the world coordinate system: The first point is given by the world coordinates of the last scanner mirror (x_1, y_1, z_1) , which are determined by the experimental setup. Two other points are the starting point $(x_2, y_2, z_2=0)$ and the final point $(x_3, y_3, z_3=0)$ of the scan vector (on top of the table), which are calculable with Eq. (4). Hence Eq. (5) gives the light plane in the usual three-point-

formulation for a plane

$$\begin{pmatrix} x \\ y \\ z \end{pmatrix}_w = \begin{pmatrix} x_1 \\ y_1 \\ z_1 \end{pmatrix}_w + \mu \begin{pmatrix} x_2 - x_1 \\ y_2 - y_1 \\ -z_1 \end{pmatrix}_w + \nu \begin{pmatrix} x_3 - x_1 \\ y_3 - y_1 \\ -z_1 \end{pmatrix}_w \quad (\mu, \nu \in \mathbb{R}) \quad (5)$$

DETECTION OF THE PROFILE

The second geometrical locus is calculable from a profile position in the computer image by doing the coordinate transformations of all steps through the detecting system. Normally, the forward transformations (according to light propagation) from workpiece surface in world coordinates $(x, y, z)_w$ to the computer image in frame grabber coordinates $(x, y)_f$ are discussed. This chapter will show the inverse transformations from a given position in the computer image to a ray in world coordinates, which accords to the given position in the computer image.

The detection of the profile comprises two imaging steps. First step is optical imaging of the profile onto the CCD sensor, second step electro-optical imaging from the sensor into the frame storage of the host computer.

Transforming computer image to sensor coordinates

Starting from a given position $(f_x, f_y)_f$ in the computer image the first step is calculation of the according position $(p_x, p_y)_c$ on the CCD sensor of the camera.

Camera and frame grabber are connected according to the CCIR video standard. Therefore frame grabber pixels and CCD sensor elements have no definite correlation and different scale factors for x- and y-coordinates must be applied. The image is transmitted line by line and the vertical scale factor is given by the vertical distance d_y of sensor elements. The different number of sensor elements N_{sx} and frame grabber pixels N_{fx} in each line cause a horizontal scale factor, which is different from the horizontal distance d_x of adjacent sensor elements. The transformation formulae from a point $(f_x, f_y)_f$ in the computer image to the corresponding point $(p_x, p_y)_c$ on the CCD sensor are given by Eq. (6)

$$\begin{pmatrix} p_x \\ p_y \\ p_z \end{pmatrix}_c = \begin{pmatrix} (f_x - C_x) d_x \frac{N_{sx}}{N_{fx}} \\ (f_y - C_y) d_y \\ z_0 \end{pmatrix}_c \quad (6)$$

where:

d_x, d_y distances of sensor elements
 C_x, C_y optical axis of the sensor (in computer image coordinates)
 N_{sx}, N_{fx} Number of pixels in each horizontal line of sensor or frame grabber
 z_0 focal distance between CCD sensor and objective ($z_0 < 0$)

The center coordinates C_x, C_y denote the position of the optical axis of the sensor in frame grabber coordinates. They are evaluated applying the direct optical method described in [10]. This method is similar to autocollimation. A He-Ne laser beam is pointed at the front lens of the camera's objective. Then the camera is adjusted in this way, that all reflected beams (caused by multiple reflections on all optical surfaces of the lens assembly) coincide with the primary laser beam. The laser beam is now aligned with the optical axis of the camera (the z_c -axis) and the computer image coordinates of the laser beam are the center coordinates C_x, C_y .

In the presented system, the use of a He-Ne laser for the autocollimation procedure has a great advantage. A bandpass interference filter is built into the CCD camera (between objective and CCD sensor) to suppress ambient light. This filter passes only laser diode wavelength and attenuates He-Ne laser wavelength significantly ($< 10^{-4}$). Hence the He-Ne laser beam can be imaged on the CCD sensor without any additional attenuation filter, which

probably would cause distortions or lateral shifts of the He-Ne laser's image and, as a consequence, errors in the evaluation of the coordinates C_x, C_y .

Transforming a sensor position to a ray

Next step is the transformation of a point on the CCD sensor (given by Eq. (6)) to the corresponding ray in world coordinates. The transformation is based on the simple principle of perspective projection with pinhole camera geometry. Hence the corresponding ray for a position $P(p_x, p_y, p_z)_c$ on the sensor is the straight line from this sensor position through the origin $O(0, 0, 0)_c$ of the camera coordinate system (which is the principal point of the objective). Hence the two-point formulation of the ray in camera coordinates is given by Eq. (7)

$$\begin{pmatrix} x \\ y \\ z \end{pmatrix}_c = \begin{pmatrix} 0 \\ 0 \\ 0 \end{pmatrix}_c + \lambda \begin{pmatrix} p_x \\ p_y \\ p_z \end{pmatrix}_c \quad (\lambda \in \mathbb{R}) \quad (7)$$

Transforming camera to world coordinates

Perspective projection transforms straight lines to straight lines. Hence the transformation of a ray can be done by individually transforming the two determining points $O(0, 0, 0)_c$ and $P(p_x, p_y, p_z)_c$ into the world coordinate system. The transformation of any point $(x, y, z)_c$ from camera coordinate system $\{x_c, y_c, z_c\}$ to world coordinate system $\{x_w, y_w, z_w\}$ given by the well-known Eq. (8)

$$\begin{pmatrix} x \\ y \\ z \end{pmatrix}_w = \begin{pmatrix} \cos(x_w x_c) & \cos(y_w x_c) & \cos(z_w x_c) \\ \cos(x_w y_c) & \cos(y_w y_c) & \cos(z_w y_c) \\ \cos(x_w z_c) & \cos(y_w z_c) & \cos(z_w z_c) \end{pmatrix} \begin{pmatrix} x \\ y \\ z \end{pmatrix}_c + \begin{pmatrix} t_x \\ t_y \\ t_z \end{pmatrix}_w \quad (8)$$

where the components of the Eulerian rotation matrix are the direction cosines of the base vectors of the coordinate systems. The translation vector shows from new origin O_w to old origin O_c , and is identical with the translation vector of camera origin in world coordinates.

Finally, the ray in world coordinates, which corresponds to the point $P(p_x, p_y, p_z)_c$ on the CCD sensor, resp. the point $(f_x, f_y)_f$ in the computer image, is determined by the two transformed points P_w and O_w in Eq. (9)

$$\begin{pmatrix} x \\ y \\ z \end{pmatrix}_w = \begin{pmatrix} t_x \\ t_y \\ t_z \end{pmatrix}_w + \lambda \begin{pmatrix} \cos(x_w x_c) & \cos(y_w x_c) & \cos(z_w x_c) \\ \cos(x_w y_c) & \cos(y_w y_c) & \cos(z_w y_c) \\ \cos(x_w z_c) & \cos(y_w z_c) & \cos(z_w z_c) \end{pmatrix} \begin{pmatrix} p_x \\ p_y \\ p_z \end{pmatrix}_c \quad (9)$$

Eq. (9) gives the world coordinates for one geometrical locus of the profile. The intersection of this ray with the light plane generated by the scanner will give 3-D world coordinates of one point of the workpiece surface.

Intersection of imaging ray and light plane

The calculation of intersection point between the illuminating light plane according to Eq. (5) and the imaging ray according to Eq. (9) is done by equating both formulae.

$$\begin{pmatrix} x_1 \\ y_1 \\ z_1 \end{pmatrix}_w + \mu \begin{pmatrix} x_2 - x_1 \\ y_2 - y_1 \\ -z_1 \end{pmatrix}_w + \nu \begin{pmatrix} x_3 - x_1 \\ y_3 - y_1 \\ -z_1 \end{pmatrix}_w = \begin{pmatrix} t_x \\ t_y \\ t_z \end{pmatrix}_w + \lambda \begin{pmatrix} \cos(x_w x_c) & \cos(y_w x_c) & \cos(z_w x_c) \\ \cos(x_w y_c) & \cos(y_w y_c) & \cos(z_w y_c) \\ \cos(x_w z_c) & \cos(y_w z_c) & \cos(z_w z_c) \end{pmatrix} \begin{pmatrix} p_x \\ p_y \\ p_z \end{pmatrix}_c \quad (10)$$

This system of linear equations leads to fixed values for λ, μ and ν , which give the 3-D coordinates of the intersection point after insertion into Eq. (9) (or, alternatively into Eq. (5)).

The above formalism gives 3-D coordinates of one point of the workpiece surface for each profile position in the computer image, i.e. one point for each line or column of computer image.

EXPERIMENTAL SETUP WITH HIGH SYMMETRY

Transformations for evaluation of 3-D data become much easier for the special case of measuring bending angles in a setup with high symmetry. This setup is characterized by the following assumptions, which can be easily fulfilled by the experimental setup:

- 1) The center of the scanner field on the surface of the optical bench defines the origin of the world coordinate system.
- 2) The profile is taken along the y_w -axis, i.e. the light plane is identical to the y_w - z_w -plane and Eq. (5) simplifies to $x_w=0$.
- 3) The origin of the camera coordinate system lies in the x_w - z_w -plane, i.e. $t_y = 0$. The mechanical adapters of scanner and camera to the optical bench are constructed to fulfil this condition.
- 4) The optical axis of the camera is directed on the origin of the world coordinate system.

Eq. (6)-(7) do not change, but transformation formula Eq. (8) from camera coordinates to world coordinates simplifies. Assumption 3) and 4) allow the description of camera orientation by only one angle ϑ and the translation vector $T(t_x, t_y, t_z)$. The angle ϑ denotes the angle between z_w -axis and $(-z_c)$ -axis, which is identical to the triangulation angle Θ in this setup. Hence Eq. (9) can be rewritten as

$$\begin{pmatrix} x \\ y \\ z_w \end{pmatrix} = -\lambda \begin{pmatrix} -\cos\vartheta & 0 & \sin\vartheta \\ 0 & 1 & 0 \\ \sin\vartheta & 0 & \cos\vartheta \end{pmatrix} \begin{pmatrix} p_x \\ p_y \\ z_0 \end{pmatrix} + \begin{pmatrix} t_x \\ 0 \\ t_z \end{pmatrix} \quad (\lambda \in \mathbb{R}) \quad (11)$$

Considering assumption 2), the parameter λ is determined by Eq. (12)

$$\lambda = \frac{-t_x}{p_x \cos\vartheta - z_0 \sin\vartheta} \quad (12)$$

Finally the 3-D coordinates of the point of the workpiece, which correspond to the position $(f_x, f_y)_f$ in the computer image, resp. (p_x, p_y, p_z) according to Eq. (6), are given by Eq. (13)

$$\begin{pmatrix} x \\ y \\ z_w \end{pmatrix} = \begin{pmatrix} 0 \\ \frac{t_x p_y}{p_x \cos\vartheta - z_0 \sin\vartheta} \\ \frac{t_x (p_x \sin\vartheta + z_0 \cos\vartheta)}{p_x \cos\vartheta - z_0 \sin\vartheta} + t_z \end{pmatrix} \quad (13)$$

The result of Eq. (13) was gained with the very simple model of perspective projection and many other influences (for example lens distortions) have been totally neglected. Suitable experiments will show the limits of this simple model, which can lead to a basic understanding of photogrammetric considerations, even if the model proves to be insufficient. It is very likely, that this model has to be improved to fit the requirements for measuring bending angles.

EXPERIMENTAL RESULTS

First measurements with the symmetrical experimental setup show promising results. Fig. 8 shows plotted profile data for a symmetrically bent sheet metal (material: St 1403, size: 200 mm x 50 mm x 2,0 mm) with a bending angle of $89^\circ 53'$ (measured with a standard mechanical goniometer). Camera coordinates were $t_x = 559$ mm and $t_z = 805$ mm, i.e. the triangulation angle was $\Theta = 34.8^\circ$. For imaging a usual 1:1.8/50 mm TV objective was used. From working distance and focus length of the objective the focal distance was calculated to $z_0 = -52.7$ mm.

Plotted in Fig. 8 are profile positions in each

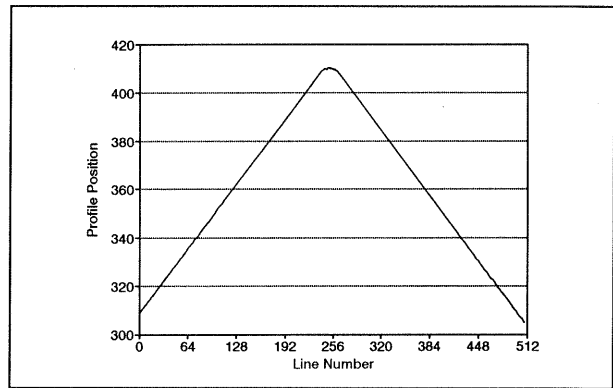


Fig. 8: Result of the off-line setup

line vs. line number, resp. x_f -coordinates vs. y_f -coordinates of the computer image. The positions are evaluated with subpixel accuracy using the Gaussian interpolation algorithm according to Eq. (1)-(3). Measuring of the bending angle requires calculation of the intersection angle of the two legs of the profile in world coordinates. The following procedure will give this angle:

First step is regression analysis for each leg of the profile in the computer image. For linear regression analysis in each leg of the profile a number of 250 data can be used. The standard deviation of evaluated profile positions from the regression line is about 0.16 pixels. This is a rather poor accuracy for Gaussian interpolation with a systematic error of about 0.01 pixels. But fortunately the profile data are centered very good around the regression line and the deviations show statistical behaviour. Hence linear regression is a very effective tool for eliminating statistical deviations from column to column and the slope of each regression line can be calculated with a standard deviation of only $1.5 \cdot 10^{-4}$ rad (resp. $1/2'$).

For the next step any two points $(A_x, A_y)_f$ and $(B_x, B_y)_f$ of each regression line are transformed into the world coordinate system according to the formalism of Eq. (6)-(13). The straight line through these two points represents the regression line in world coordinates. Essential for evaluating the bending angle is the slope of this straight line, which is given by Eq. (14)

$$\frac{z_B - z_A}{y_B - y_A} = - \frac{B_x - A_x}{(A_x B_y - A_y B_x) \frac{\cos\vartheta}{z_0} + (B_x - A_x) \sin\vartheta} \quad (14)$$

Last step is the calculation of the bending angle from the two slopes for the regression lines for each leg of the workpiece. Application of Eq. (14) for the data of Fig. 8 yields to slopes for legs of the workpiece of 44.80° and -45.08° , from which the bending angle is easily inferred to 89.88° or $89^\circ 53'$, which is exactly the same value as measured by the mechanical goniometer.

The simple model of the detection system yields to a measuring accuracy of the bending angle, which is comparable with conventional mechanical goniometers. In despite of this promising result there probably might be more calibration efforts necessary, if the system must deal with any given experimental setup.

ERRORS AND ITS SOURCES

The CCIR standard video interface between camera and frame storage is suggested to be the main source of error. Different authors have investigated the electronic transfer chain from CCD sensor to frame storage in detail (see for example [5], [11]). The analogous video signal in combination with the lack of standards for the number of pixels in a horizontal line cause statistical deviations in the synchronization of the frame grabber's A/D-converter, the so-called line jitter. In combination with the different number of 756 sensor elements and 512 frame storage pixels there is no

definite and precise relation between sensor elements and frame storage pixels.

Hence electronic insufficiencies in conventional CCIR standard video interfaces destroy the advantage of geometric stable CCD sensor elements. A typical value for jitter is 20 ns, which will cause statistical deviations of about 0.2 pixel in profile positions from line to line. This value corresponds very well to the experimentally gained values for the standard deviation of profile positions around the regression line.

The solution of this problem follows a simple principle: pixel clock signals from the CCD sensor must be transmitted to the frame storage. Fortunately more and more manufacturers of cameras and frame storage boards get rid of the conventional CCIR video standard and offer pixel-synchronous image acquisition systems. Applications of pixel-synchronous image acquisition systems report subpixel resolutions of 1% to 3% of a pixel period [12], [13]. This resolution is about 10 times higher than the reported resolutions for CCIR standard image acquisition systems [5], [14], [15].

CONCLUSIONS

The industrial application of an optical 3-D sensing method requires careful considerations about system design. Especially the condition of a scanning illumination system influences the criteria for the choice of a CCD camera for the detection system.

Evaluation of 3-D data from the camera image demands for the application of photogrammetric methods for calibration of the detection system. The basic equations for a simple camera model of perspective projection with pinhole imaging are derived. The results gained with the experimental setup with high symmetry show promising results even for this simple model.

The analysis of the observed errors shows again the importance of pixel synchronous image acquisition.

In spite of this avoidable errors, the accuracy of the optical 3-D sensor is comparable with usual industrial measuring methods, which can not be used for an in-process measurement. Thus the presented non-contact, simple and fast optical 3-D sensor based on the principle of light sectioning meets all requirements for the in-process measurement of bending angles.

ACKNOWLEDGEMENTS

The investigations presented in this paper are carried out at the University of Erlangen-Nürnberg, Chair of Manufacturing Technology, and supported by the 'Deutsche Forschungsgemeinschaft' (Ref.: Ge 530/6-1, 'Biegewinkel erfassung').

The author would like to thank his professor in ordinary, Univ.-Prof. Dr.-Ing. Manfred Geiger, for the opportunity to work on this project and for his scientific advice and confidence.

REFERENCES

- [1] Häusler, G.; Heckel, W.: Light sectioning with large depth and high resolution. *Applied Optics*, Vol. 27 (1988), No. 24, p. 5165.
- [2] McLeod, J.H.: Axicon: A new type of optical element. *J. Opt. Soc. Am.*, Vol. 44 (1954), p. 592.
- [3] McLeod, J.H.: Axicons and their uses. *J. Opt. Soc. Am.*, Vol. 50 (1960), p. 166.
- [4] Slevogt, H.: *Technische Optik*. Berlin: de Gruyter, 1974, p. 56.
- [5] Lenz, R.: Zur Genauigkeit der Videometrie mit CCD-Sensoren. In: *Proc. DAGM = Informatik Fachberichte 180*, Vol. 10 (1988), p. 179.
- [6] Alexander, B.F.; Ng, K.C.: Elimination of systematic error in subpixel accuracy centroid estimation. *Optical Engineering*, Vol. 30 (1991) 9, p. 1320.
- [7] Seitz, P.: Optical superresolution using solid-state cameras and digital signal processing. *Optical Engineering*, Vol. 27 (1988) 7, p. 535.
- [8] Heckel, W.: *Lichtschnittverfahren mit erweitertem Meßbereich und hoher Auflösung*. Diploma Thesis, University of Erlangen, Physics Institute, 1988.
- [9] Tsai, R.Y.: A versatile camera calibration technique for high accuracy 3D machine vision metrology using off-the-shelf TV cameras and lenses. *IBM Research Report RC 11414 (#51342)*, 1985.
- [10] Lenz, R.K.; Tsai, R.Y.: Techniques for calibration of the scale factor and image center for high accuracy 3D machine vision metrology. *IBM Research Report RC 12266 (#54867)*, 1986.
- [11] Dähler, J.: Problems in digital image acquisition with CCD cameras. *Proc. of ISPRS Intercommission Conf. on "Fast processing of photogrammetric data"*, Interlaken, June 2-4, 1987, p. 48.
- [12] Raynor, J.M.; Seitz, P.: The technology and practical problems of pixel-synchronous CCD data acquisition for optical metrology applications. *Proc. SPIE*, Vol. 1395 (1990), p. 96.
- [13] Gale, M.T.; Seitz, P.: High resolution optical metrology and edge detection using a PC-controlled smart CCD Camera. *Proc. SPIE*, Vol. 701 (1986), p. 254.
- [14] Hachicha, A.; Simon, S.: Subpixel edge detection for precise measurements by a vision system. *Proc. SPIE*, Vol. 1010 (1988), p. 148.
- [15] Kleinemeier, B.: Measurement of CCD interpolation functions in the subpixel precision range. *Proc. SPIE*, Vol. 1010 (1988), p. 158.